

# Local refinement of a national-scale groundwater model

Julian Koch\*, Jun Liu & Lars Trolborg

Geological Survey of Denmark and Greenland, Department of Hydrology, Copenhagen,  
Denmark

\*juko@geus.dk

## Abstract

This method article presents a local refinement framework for a national-scale, machine learning-based groundwater model that predicts typical summer and winter water table depth at  $10 \times 10$  m resolution at national scale of Denmark. While the existing baseline model provides high-resolution national coverage and is suitable for screening purposes, its accuracy remains insufficient for local groundwater management applications. The proposed method integrates new groundwater observations into the existing training dataset and retrains the baseline model to enhance local fidelity while preserving large-scale consistency. The approach is demonstrated for a 212 km<sup>2</sup> case study area using 100 synthetic groundwater observations. Cross-validation results show consistent improvements in mean error, mean absolute error, and root mean squared error compared to the baseline model, particularly when increased weights are assigned to new observations. The refined models produce improved precision in areas with new observations while maintaining baseline behaviour elsewhere, demonstrating its suitability for combining national datasets with local monitoring networks for improved decision support in climate adaptation, nature conservation and other applications.

## 21 Introduction

22 This method builds upon the national-scale machine learning-based groundwater model  
23 developed by Koch et al. (2021), which predicts typical summer and winter water table depth at  
24 10 × 10 m resolution across Denmark. The model targets the uppermost groundwater table and  
25 generates high-resolution map products that are distributed through the Hydrological  
26 Information and Prognosis system (HIP, <https://hipdata.dk/>). The 10 m maps provide a valuable  
27 screening resource for Danish municipalities, water utilities and other decision makers for  
28 planning climate adaptation measures, particularly in relation to flood risk. The datasets are for  
29 example highlighted in the EPA’s climate adaptation implementation (Danish EPA, 2025). Despite  
30 the high spatial resolution and overall improved precision compared to the process-based  
31 national hydrological model of Denmark (DK-model, Henriksen et al. (2022)), which operates at  
32 100 m resolution, the 10 m models still lack sufficient accuracy to support local groundwater  
33 management decisions. Examples include expanding drainage capacities in urban areas or nature  
34 restoration planning involving groundwater-surface water interactions. The mean absolute error  
35 of the 10 m national baseline model is approximately 1 m, which may limit its applicability for  
36 local decision-making.

37 With increasing awareness of shallow groundwater challenges concerning flood resilience,  
38 irrigation planning, and nature conservation, together with the availability of cost-effective  
39 groundwater monitoring systems, many decision makers have invested in local groundwater  
40 monitoring networks. However, the integration of these point observations into spatial  
41 groundwater modelling workflows remains challenging and requires specialised technical  
42 expertise. The presented method aims to address this gap by equipping decision makers with a  
43 practical workflow for incorporating local groundwater observations into a state-of-the-art  
44 machine learning modelling framework. The method enables the generation of high-resolution  
45 maps of groundwater dynamics by combining national-scale databases with locally collected  
46 groundwater observations through machine learning models.

## 47 Resources required

48 The required resources are as follows:

- 49 • Sufficient computing environment (~25 Gigabyte RAM, not GPU dependent).
- 50 • Python 3.12 including the following packages, numpy, pandas, pyarrow, lightgbm, scikit-  
51 learn, gdal, geopandas, pyproj, shapely and fiona. Required versions are further specified  
52 in the environment.yml file available via Koch (2026b).
- 53 • Input data for machine learning model, *df\_predcit.parquet* is available via Koch (2026a)  
54 and *df\_train.parquet* is available via Koch (2026b).
- 55 • Auxiliary data and code provided by Koch (2026a, 2026b).
- 56 • Local groundwater observations representing typical winter and summer conditions.

## 57 Methodological protocols

### 58 Curating groundwater observations

59 New groundwater observations are the core input driving the local model refinement. The  
60 method requires a CSV file containing ETRS89 / UTM 32N coordinates (EPSG: 25832) together

61 with median summer and winter water table depths. Users are responsible for curating these  
62 medians given uncertainties in the underlying data, including short time series and well screen  
63 placement, as the model assumes that the well screen represents the uppermost groundwater  
64 table. Shallow wells can be identified through a combination of depth criteria-based lithology and  
65 the homogeneity of the lithostratigraphy of the well. The training data for the baseline model  
66 contains observations from the period 1991 to 2025. Both summer and winter groundwater  
67 levels must be provided. If only one seasonal estimate is available, users are encouraged to  
68 estimate the seasonal amplitude to derive the missing season. Summer medians should  
69 represent June to August, whereas winter medians should represent December to February.  
70 Further details regarding preprocessing are provided by Koch et al. (2021). The training data used  
71 to build the national baseline model are provided (`df_train.parquet`), and users are encouraged  
72 to explore which groundwater observations are already included in the national dataset using  
73 the available coordinates or the provided shapefile of the training data location and metadata.  
74 To demonstrate the method, 100 synthetic summer and winter observations were generated and  
75 are provided in Koch et al. (2021).

#### 76 [Retraining machine learning model](#)

77 The local refinement is performed by retraining the underlying machine learning model. First,  
78 covariate data are extracted for the newly provided groundwater observations. The  
79 computational efficiency of this step depends on the size of the user-defined prediction domain.  
80 The model incorporates 22 covariates, which are specified by Koch et al. (2021) and Troldborg at  
81 al. (2026). After extraction, the covariate data are concatenated with the existing training dataset  
82 (`df_train.parquet`). Subsequently, the summer and winter models, including their associated  
83 uncertainty models (`q10` and `q90`), are retrained using the predefined hyperparameters. Existing  
84 training observations may also be removed if they are considered unreliable or uncertain by the  
85 user. This can be done by dropping specific rows from the training dataframe. We advise users  
86 to explore the training data through the provided shapefile where the wells can be linked to the  
87 the training dataframe using the `WELLID` column.

88 The newly added observations can be assigned additional influence during model training in two  
89 different ways, which can be controlled by parameters “`weight_local`” and “`repeat_local`” in the  
90 main script (`main.py`). The motivation is to force the machine learning model towards improved  
91 local accuracy while still retaining the large-scale relationships learned from the national dataset.  
92 The first option is data augmentation, where local observations are duplicated multiple times in  
93 the training dataset. The second option is weight assignment, where local observations are  
94 assigned higher weights in the loss function. By default, synthetic observations are assigned a  
95 weight of 1, while groundwater wells are assigned a weight of 2. Additional details are provided  
96 in Koch et al. (2021). The sensitivity of the two parameters will depend on the size of the new  
97 groundwater observations and how they agree with the baseline training data and therefore we  
98 encourage users to explore the sensitivity from case to case.

#### 99 [Model validation and prediction](#)

100 In the provided scripts, the local refinement is evaluated using 4-fold cross-validation. Validation  
101 focuses specifically on the newly provided groundwater observations. First, a baseline model is

102 trained exclusively on the pre-existing national-scale training data, excluding the new  
103 observations. Subsequently, four refined models are trained including the new observations. The  
104 cross-validation scheme ensures that, for each model, 25% of the new observations are used for  
105 testing while 75% are used for training. In this way, each local observation is used exactly once  
106 for validation. By default, mean error (ME), mean absolute error (MAE), and root mean squared  
107 error (RMSE) are calculated and their mean value is calculated across the four validation folds.  
108 Validation is carried out separately for the summer and winter models.

109 In total, six models are trained, each generating  $10 \times 10$  m water table depth maps. Predictions  
110 are produced for the local prediction domain specified by the user. Hyperparameters remain  
111 fixed during refinement, ensuring that model improvements are driven solely by the inclusion of  
112 the new groundwater observations. The outputs include predictions of typical summer and  
113 winter water table depth, together with two uncertainty bounds for each model: the 10th  
114 percentile (q10), representing the shallow bound, and the 90th percentile (q90), representing the  
115 deep bound. Together, these approximate an 80% confidence interval. All prediction maps are  
116 exported as GeoTIFF files and represent water table depth in cm below ground level.

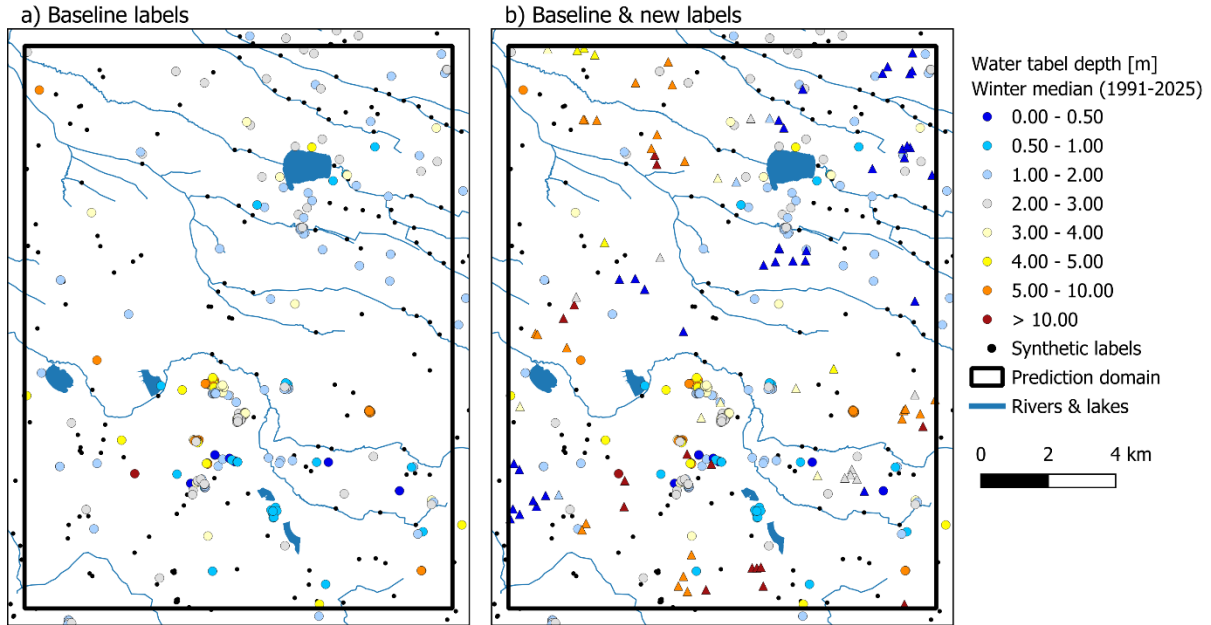
#### 117 [Auxiliary outputs](#)

118 In addition to the six prediction maps, several auxiliary outputs are generated. The 22 covariate  
119 raster layers are clipped to the local prediction domain and exported as GeoTIFFs. Furthermore,  
120 the training data are exported as a point shapefile covering the prediction domain. User-provided  
121 groundwater observations are labelled with "user" in the attributes TYPE and WELLID.

## 122 [Demonstration](#)

### 123 [Validation on synthetic data](#)

124 The presented method is demonstrated for an area surrounding the city of Sunds in Jutland with  
125 a simulation domain of approximately 212 km<sup>2</sup>. A total of 100 synthetic groundwater  
126 observations were generated. Figure 1a illustrates the baseline training labels representing the  
127 national-scale training dataset also used in HIP. This dataset includes both in situ groundwater  
128 observations and synthetic labels representing expert-generated groundwater conditions along  
129 rivers, groundwater-connected lakes, and coastline. In addition, the 100 local observations used  
130 for refinement are shown in Figure 1b. Spatial clustering and comparable groundwater depth  
131 values are evident, reflecting the characteristics typically found in real-world monitoring  
132 datasets.



133  
134  
135  
136  
Figure 1. Observations of water table depth under typical winter conditions used as training labels for a) the national-scale baseline model shown as circles and b) the local model refinement shown as triangles. The training dataset also includes synthetic labels representing rivers and lakes.

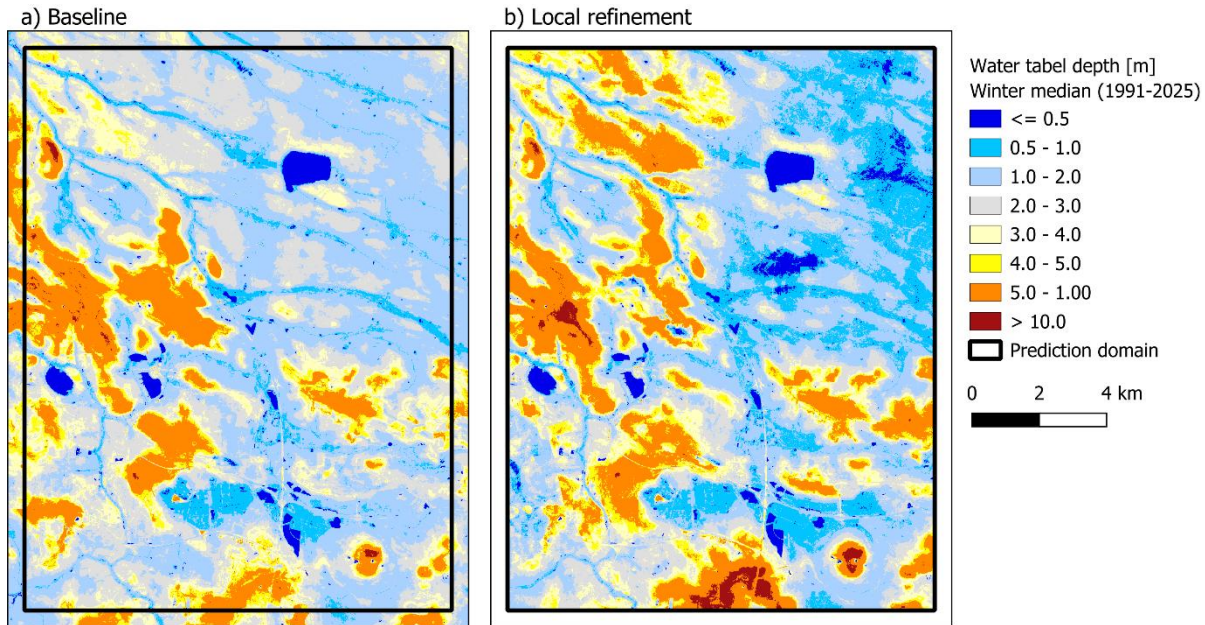
137 Results from the 4-fold cross-validation using the 100 synthetic groundwater observations are  
138 presented in Table 1. Compared with the national-scale baseline model, all three performance  
139 metrics indicate improved model performance following local refinement. For both MAE and  
140 RMSE, model precision further improved when increasing the weight assigned to the new  
141 groundwater observations from 2 to 5 during training. This indicates that stronger weighting of  
142 local observations can enhance local model performance. It should be noted that the validation  
143 labels are synthetic, and therefore the practical implications of the reported performance metrics  
144 should not be overinterpreted. Nevertheless, the relative differences between the evaluated  
145 modelling scenarios clearly demonstrate the usability and functionality of the presented method.

146  
147  
148  
149  
Table 1. 4-fold cross-validation of the 100 synthetic groundwater observations (Figure 1b). Mean error (ME), mean absolute error (MAE), and root mean squared error (RMSE) for summer (s) and winter (w) groundwater predictions from the national-scale baseline model and two locally refined models. The local refinements were performed using two different weighting parameters (w) for the newly added groundwater observations.

	Baseline		Local refinement (w=2)		Local refinement (w=5)	
	s	w	s	w	s	w
ME [m]	-0.86	-1.08	-0.62	-0.77	-0.66	-0.77
MAE [m]	3.64	3.96	2.88	2.91	2.73	2.76
RMSE [m]	4.34	4.79	3.56	3.64	3.44	3.54

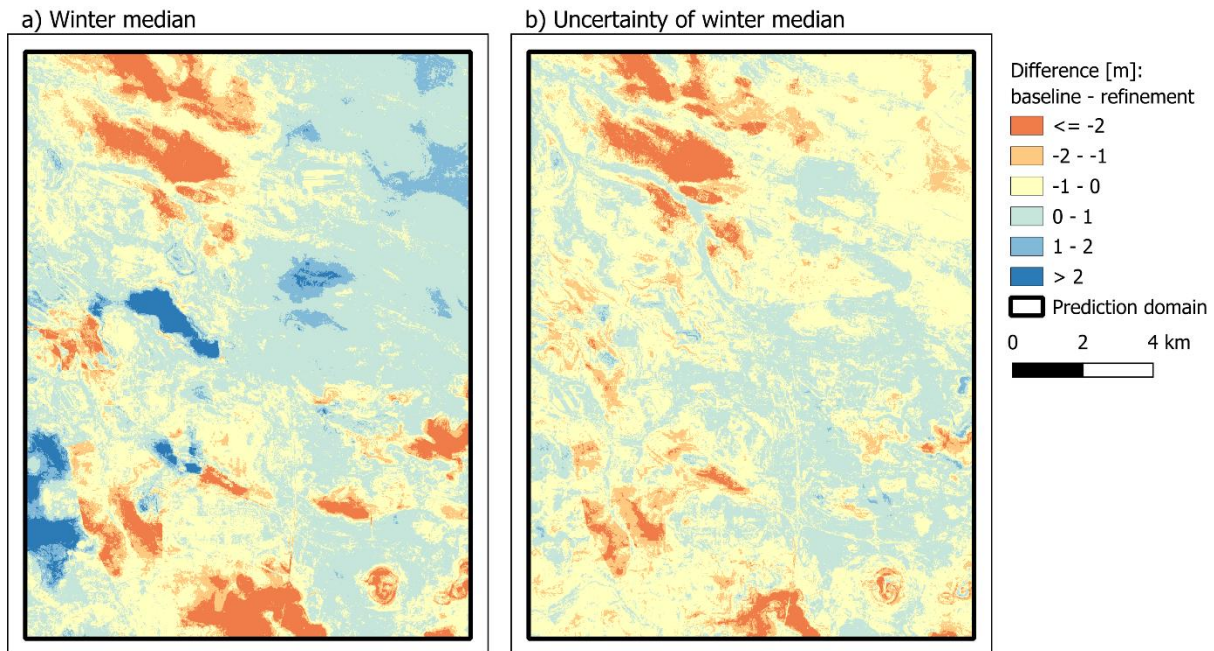
150 The resulting maps of typical winter conditions for the baseline model and the locally refined  
151 model are presented in Figure 2. The local refinement differs from the baseline model in  
152 accordance with the synthetic groundwater observations added during training. For example, a

153 cluster of deep groundwater observations has a pronounced influence in the north-western part  
 154 of the prediction domain, resulting in deeper predicted groundwater levels. Similarly, the shallow  
 155 groundwater observations introduced in the north-eastern part of the domain lead to overall  
 156 wetter predicted conditions. It is also noteworthy that areas without additional observations, or  
 157 areas where the added observations are consistent with the baseline model, remain largely  
 158 unchanged after local refinement. This indicates that the refinement primarily affects locations  
 159 supported by new observations while preserving the large-scale spatial patterns of the baseline  
 160 model.



161  
 162 *Figure 2. a) The baseline model derived from the existing national-scale training dataset, identical to the data distributed via HIP*  
 163 *(<https://hipdata.dk/>). (b) The local refinement obtained from a retrained model incorporating 100 new groundwater observations*  
 164 *(Figure 1b). Both maps represent typical winter groundwater conditions for the period 1991-2025.*

165 This is further exemplified in Figure 3, where the differences between the baseline model and  
 166 the refined model are shown. The spatial patterns of positive and negative differences in Figure  
 167 3a correspond well with the distribution of newly added deep and shallow observations,  
 168 respectively, as illustrated in Figure 1b. Uncertainties, expressed as the width of the confidence  
 169 interval ( $q_{90} - q_{10}$ ), are compared between the baseline and refined models in Figure 3b.  
 170 Uncertainties are generally higher in areas where the refined model predicts a deeper  
 171 groundwater table, whereas lower uncertainties are associated with areas with shallower  
 172 groundwater conditions in the refined model. This indicates that uncertainty scales with  
 173 groundwater depth; however, further investigations using real observations are required to draw  
 174 robust conclusions. Theoretically, a higher density and improved quality of local observations  
 175 should lead to an overall reduction in uncertainty.



176

177 *Figure 3. a) Spatial distribution of differences between the baseline model and the locally refined model (baseline - local*  
 178 *refinement). b) Comparison of uncertainty between the baseline and refined model, expressed as the width of the 80% confidence*  
 179 *interval (q90–q10).*

## 180 Acknowledgements

181 n/a

## 182 References

183 Danish EPA. (2025). Tillæg til spildevandsvejledningen: Kommunernes planlægning for  
 184 terrænnært grundvand. Vejledning, nr. 83. Miljøstyrelsen.  
 185 <https://www2.mst.dk/Udgiv/publikationer/2025/12/978-87-7564-074-4.pdf>

186

187 Henriksen, H. J., Schneider, R., Koch, J., Ondracek, M., Troldborg, L., Seidenfaden, I. K., ... & Stisen,  
 188 S. (2022). A new digital twin for climate change adaptation, water management, and disaster risk  
 189 reduction (HIP digital twin). *Water*, 15(1), 25.

190

191 Koch, J., Gotfredsen, J., Schneider, R., Troldborg, L., Stisen, S., & Henriksen, H. J. (2021). High  
 192 resolution water table modeling of the shallow groundwater using a knowledge-guided gradient  
 193 boosting decision tree model. *Frontiers in Water*, 3, 701726.

194

195 Koch, J. (2026a). Dataframe for 10 m water table depth predictions at DK-scale [Data set]. GEUS  
 196 Dataverse. <https://doi.org/10.22008/FK2/DUU3WM>

197

198 Koch, J. (2026b). RefineWTD10m [Source code]. GEUS GitLab. Retrieved May 19, 2026, from  
 199 <https://geusgitlab.geus.dk/hydrology-public/RefineWTD10m>

200

201 Troldborg, L., Ondracek, M., Koch, J., Schneider, R. J. M., Henriksen, H. J., Kragh, S. J., Gotfredsen,  
 202 J., van Til, M., Jakobsen, A., Rasmussen, P., Pasten-Zapata, E., & Stisen, S. (2026).

203 Dokumentationsrapport vedr. modelleverancer til Hydrologisk Informations- og Prognosesystem  
204 – Version 2 (GEUS Rapport 2026/9). De Nationale Geologiske Undersøgelser for Danmark og  
205 Grønland. <https://doi.org/10.22008/gpub/38964>